Journal of Magnetic Resonance **138,** 28–35 (1999)
Article ID jmre.1999.1723, available online at http://www.idealibrary.com on IDEAL®

^{13}C NMR of Liquid Crystals with Different Proton Homonuclear Dipolar Decoupling Methods

B. M. Fung, Konstantin Ermolaev,[1] and Youlu Yu[2]

Department of Chemistry and Biochemistry, University of Oklahoma, Norman, OK 73019-0370

Received September 15, 1998; revised January 26, 1999

The effect of several new homonuclear dipolar decoupling methods (frequency-switching Lee–Goldburg decoupling and two sequences based on *z*-rotational decoupling) on the ^{13}C spectra of liquid crystals has been studied, and the results are compared with those obtained by using two well-established methods (MREV-8 and BLEW-48). For benzene dissolved in two liquid crystalline solvents, BLEW-48 gives the best spectral resolution. The BLEW-48 sequence has also been applied to the 2D method of proton-encoded local field (PELF) spectroscopy to study a bulk liquid crystal, 4-*n*-pentyl-4′-cyanobiphenyl (5CB). The results are compared with those obtained by using MREV-8, and it is suggested that the BLEW-48 sequence may be preferable to MREV-8 for application in the PELF method.

INTRODUCTION

Because the molecular motions in solids and liquid crystals are strongly restricted, their NMR spectra are usually severely broadened by quadrupole coupling, dipolar coupling, or chemical shift anisotropy. Various techniques have been used to reduce or eliminate these effects to decrease the linewidths of the NMR peaks. For $I = \frac{1}{2}$ spin systems, the most prevalent line broadening is dipolar coupling; methods to reduce the linewidth include magic angle spinning, homonuclear dipolar decoupling, and broadband heteronuclear decoupling.

The earliest method of homonuclear dipolar decoupling was off-resonance "magic angle CW" (continuous wave) irradiation, proposed by Lee and Goldburg (*1*). In their approach, the radiofrequency (RF) source used to excite the spin system is set to differ from the Larmor frequency ω_0 by an offset $\Delta\omega$ that satisfies the condition $\gamma B_1/\Delta\omega = \sqrt{2}$, where B_1 is the RF field strength, so that the spin system would precess about an axis forming the magic angle ($\tan^{-1}\sqrt{2} = 54.74°$) with respect to the magnetic field B_0, and the dipolar coupling term in the effective spin Hamiltonian would vanish. However, because the Lee–Goldburg method only eliminates the dipolar interaction to the zeroth order, it is not very effective. Later on, Waugh, Huber, and Haeberlen introduced a multiple-pulse WAHUHA sequence (*2, 3*) to remove the dipolar terms in the average spin Hamiltonian up to the first order to achieve more efficient homonuclear dipolar decoupling. Since then, many other multiple-pulse dipolar-decoupling sequences have been proposed for further improvement (*4–14*). The most commonly used method is perhaps the 8-pulse MREV-8 sequence (*4, 5*). The combination of magic angle spinning and multiple-pulse dipolar decoupling (CRAMPS, *15–17*) has proven to be very useful in obtaining high-resolution proton spectra of solids. In 1989, Levitt and co-workers (*11, 12*) demonstrated that the "magic-angle CW" method of Lee and Goldburg (*1*) can be dramatically improved by frequency switching. In their approach, the frequency offset is rapidly switched from a positive value to a negative value for every 2π precession, with a concomitant 180° phase shift. It was shown that the results are comparable to or better than those of many multiple-pulse dipolar decoupling methods (*11, 12*).

We have been interested for some time in applying homonuclear dipolar decoupling to study liquid crystals (*18, 19*). The main purpose is to remove H–H dipolar coupling as much as possible, so that the splittings in the 1D and 2D ^{13}C spectra would give accurate C–H dipolar coupling constants (*20, 21*). In an earlier article (*19*), the efficiencies of a number of homonuclear dipolar decoupling sequences, including Lee–Goldburg CW (*1*), WAHUHA (*2, 3*), MREV-8 (*4, 5*), BR-24 (*6*), BR-52 (*6*), BLEW-48 (*7*), and TREV-8 (*8*), were compared. It was found that BLEW-48 gave the best performance. Since then, several new homonuclear dipolar decoupling methods have been proposed for the study of proton NMR in solids (*9–14*). In this work, we report a study on the efficiency of some of these new methods applied to the ^{13}C NMR of liquid crystals, and a comparison the results with those obtained by using the MREV-8 and BLEW-48 sequences. The use of the BLEW-48 sequence in the 2D proton-detected local field method (*22–25*) has also been examined, and the results are discussed.

EXPERIMENTAL

The liquid crystals 4-*n*-pentyl-4′-cyanobiphenyl, TNC 1291, and ZLI 1167 were obtained from EM Chemicals (Hawthorne, NY) and used without further purification.

[1] Present address: Quantum Magnetics, 7740 Kenawar Court, San Diego, CA 92121-2425.

[2] Present address: Phillips Petroleum Company, Bartlesville, OK 74004.

1090-7807/99 $30.00

All NMR experiments were carried out on a Varian UNITY/INOVA 400 NMR spectrometer. For the off-magic-angle-spinning (OMAS) experiments, the angle of the spinning axis with respect to B_0, β, was determined by studying the deuterium quadrupole splittings of a solution of $CDCl_3$ in TNC 1291; the ratio of the splittings obtained with and without rapid spinning (spinning rate ~1 kHz) is equal to $(3\cos^2\beta - 1)/2$ (*20*).

RESULTS AND DISCUSSION

Liquid Crystal Solutions

Among the homonuclear dipolar decoupling methods published before 1986, it was found that the BLEW-48 sequence gave the best results for the study of ^{13}C and ^{2}H NMR in liquid crystals (*18, 19*). Since then, other homonuclear dipolar decoupling methods have been proposed for solid-state NMR (*9–14*). Several sequences using composite pulses gave very good simulated spectra (*9*), but the results were not substantiated experimentally (*10*). For some other sequences, the performances match the theoretical predictions (*11–14*).

The frequency-switching Lee–Goldburg (FSLG-2) method (*11, 12*) has proven to be very successful for solid state NMR and has been applied to 2D studies (*26, 27*) using the separated local field (*28–31*) approach. To implement this method, the time it takes to switch the spectrometer frequency should be less than 1 μs. This requires special hardware not routinely available in commercial spectrometers. However, if T_2 of the system is not too short, such as in the cases of solids with rapid internal rotations and liquid crystals, there is an alternative way to achieve the frequency-switching effect. This is accomplished by making a discontinuous change in a linear ramp of small-angle phase of the decoupler, because the frequency jumps and phase shifts are related to each other (*32, 33*). This was the method used in our experiments.

More recently, a method based on *z*-rotational decoupling was proposed by Hohwy *et al.* (*13, 14*) to eliminate the higher order dipolar coupling terms. One of the sequences is abbreviated as MSHOT-3 for Magic Sandwich High Order Truncation, another as BHOT-4 for High Order Truncation with BLEW-12. It was shown that MSHOT-3 gave very good results for CRAMPS experiments (*13, 14*).

Because of the success of these homonuclear dipolar decoupling methods in the study of solid samples, we proceeded to test their performance for liquid crystal systems. The results of applying the FSLG-2, MSHOT-3, and BHOT-4 homonuclear decoupling methods to study the ^{13}C spectra of benzene dissolved in two liquid crystalline solvents are shown in Fig. 1. Results obtained from using the MREV-8 and BLEW-48 sequences are also displayed in the same figure for comparison. In all the experiments, a waveform generator was used to generate the desired decoupling sequence in the acquisition period, and the duty cycle was kept to only 2% to avoid significant RF heating (*34*).

The results in Fig. 1 show that all the proton–proton dipolar decoupling methods, except BHOT-4, reduce the complex ^{13}C spectrum to first order. This means that, because the ^{1}H–^{1}H dipolar interaction terms are removed from the average spin Hamiltonian, the spectrum is determined by ^{1}H–^{13}C couplings only. In each decoupled spectrum, the large splitting is due to coupling with the directly bonded (*ipso*) proton, and the triplet in each half is due to coupling with the two *ortho* protons. Couplings with the *meta* and *para* protons are resolvable in some of the spectra, and the BLEW-48 sequence gives the highest resolution.

Quantitatively, the coupled spectrum can be analyzed to obtain all the H–H and C–H dipolar coupling constants. Then, each proton–proton dipolar decoupled spectrum can be analyzed by setting the H–H dipolar coupling constants to zero and multiplying all the C–H scalar and dipolar couplings with a single scaling factor (*18*). The scaling factors calculated from the experimental spectra of benzene dissolved in two liquid crystalline solvents, TNC 1291 (anisotropy of the magnetic susceptibility $\Delta\chi > 0$) and ZLI 1167 ($\Delta\chi < 0$), are listed in Table 1. For all these methods, small variations of the carrier frequency of the decoupler (up to ~500 Hz) did not change the quality of the decoupled spectra and the scaling factor. The BHOT-4 sequence seems to give two sets of decoupled peaks with different scaling factors, but the reason for this is not clear. Therefore, the results obtained for BHOT-4 are not included in Table 1. For comparison, the theoretical scaling factors are also listed in Table 1, and they were calculated in the following way.

For the MREV-8 sequence, when pulse imperfections are neglected, the Zeeman part of the average Hamiltonian is (*5*)

$$\bar{H}_z^{(0)} = \frac{1 + 2a}{3} \sum_i (I_{xi} + I_{zi}) \cdot (\omega_0 - \omega_i), \qquad [1]$$

where

$$a = \left(\frac{4}{\pi} - 1\right) \cdot \frac{3\tau_\omega}{t_c}, \qquad [2]$$

in which τ_ω is the 90° pulse width and t_c is the cycle time. Therefore, the theoretical scaling factor $\sqrt{2}\ (1 + 2a)/3$ depends on the pulse width as well as the pulse spacing, and both can vary. For the ^{13}C spectra of benzene dissolved in the liquid crystal solutions with proton homonuclear dipolar decoupling using a waveform generator, we found that a semi-windowless version (xy–τ–$\bar{y}\bar{x}$–τ–$\bar{x}y$–τ–$\bar{y}x$–τ, where τ is set to be equal to the 90° pulse width) was most convenient and gave the best results, and the theoretical scaling factor was calculated accordingly. For BLEW-48, FSLG-2 and MSHOT-3, the theoretical scaling factors are $\frac{4}{3}\pi$ (*7*), $1/\sqrt{3}$ (*11, 12*), and $(7\pi + 8)/27\pi$ (*13, 14*), respectively. The data in

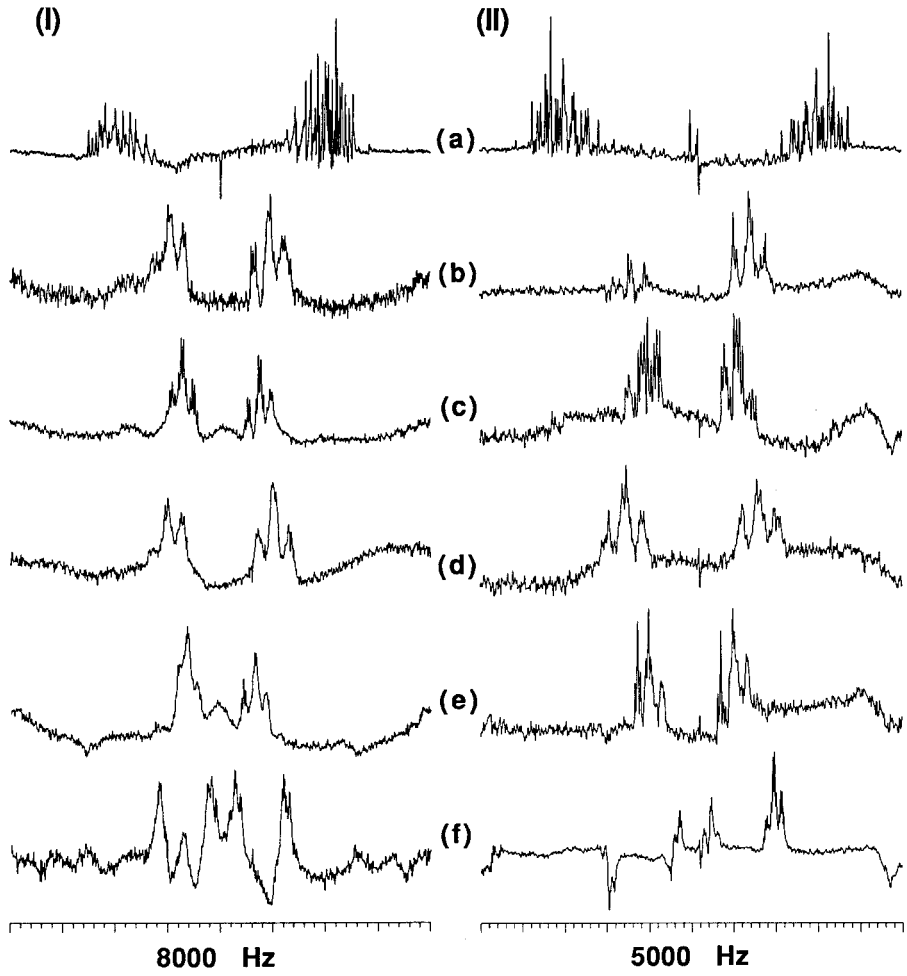

FIG. 1. ^{13}C NMR of benzene (~8%) dissolved in two liquid crystalline solvents at 9.4 T and 21°C, without and with various proton–proton dipolar decoupling methods. (a) Coupled spectra; (b) MREV-8 (*4, 5*); (c) BLEW-48 (*7*); (d) FSLG-2 (*11, 12*); (e) MSHOT-3 (*13, 14*); (f) BHOT-4 (*13, 14*). Column I: Solvent = TNC 1291 ($\Delta\chi > 0$); decoupler power $\gamma B_2/2\pi$ = 11 kHz; the first two points of the free induction decay (FID) were removed for data processing (with a line broadening factor of 5 Hz) to reduce the broad background due to the liquid crystal solvent. Column II: Solvent = ZLI 1167 ($\Delta\chi < 0$); decoupler power $\gamma B_2/2\pi$ = 10 kHz; the whole FID was used for data processing; line broadening factor = 5 Hz.

Table 1 show that experimental scaling factors for all the sequences examined are very close to the theoretical values; the experimental values for BLEW-48 are in good agreement with the value determined previously (*18*).

The lower resolution of the new FSLG-2 and MSHOT-3 methods for the case of benzene dissolved in liquid crystalline solvents (Fig. 1) does not necessarily mean that they are inferior to the BLEW-48 sequence for homonuclear dipolar decoupling. For the FSLG-2 method, it is not clear to us whether its performance is affected by the use of small phase angle ramp instead of actual frequency jumps. For the MSHOT-3 method, the pulse sequence was specially designed to eliminate higher order dipolar terms (*13, 14*) and may be more suitable for proton line narrowing of solids with magic angle spinning than applications to the study of liquid crystals. On the other hand, the long cycle time and moderate scaling factor of the BLEW-48 sequence compared to MREV-8, FSLG-2, and MSHOT-3 are disadvantageous in some applications. Furthermore, because BLEW-48 is windowless, it is inconvenient for direct application in CRAMPS experiments.

TABLE 1
Scaling Factors for Several Proton Homonuclear Dipolar Decoupling Methods

	MREV-8	BLEW-48	FSLG-2	MSHOT-3
Theoretical	0.536	0.424	0.577	0.354
Experimental, in TNC 1291	0.525	0.414	0.563	0.363
in ZLI 1167	0.533	0.414	0.568	0.357

Bulk Liquid Crystals

Because proton–proton dipolar decoupling can simplify the ^{13}C spectra to first order, it is very useful for the study of bulk

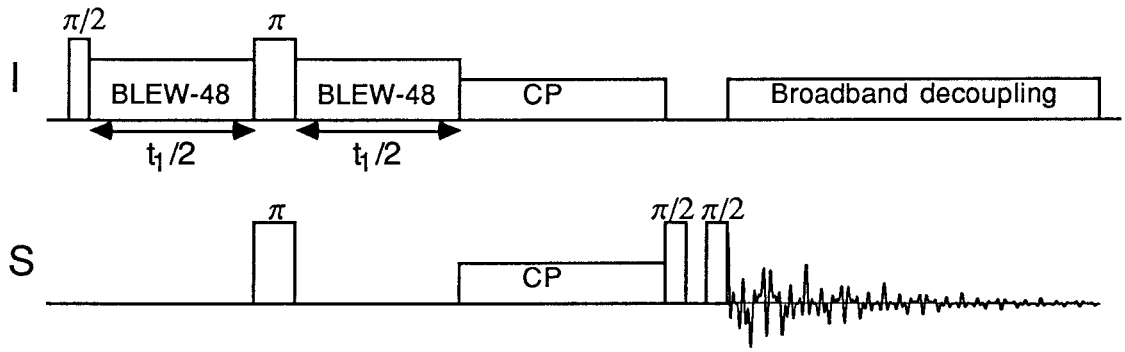

FIG. 2. A schematic diagram of the 2D proton-encoded local field (PELF) method using the BLEW-48 sequence (*7*) for proton–proton dipolar decoupling. CP = cross polarization. The last two $\pi/2$ pulses of the S spin act as a "*z*-filter." The phase cycles are listed in Table 2.

liquid crystals. By applying it to the 2D method of separated local field (SLF) spectroscopy (*28–31*), especially in combination with off-magic-angle-spinning (OMAS, *20*), C–H dipolar coupling constants of various molecular segments in a liquid crystal can be obtained from its ^{13}C spectra. This has been shown to be a very useful method to study the orientational ordering of liquid crystals (*21*). Recently, Pines and co-workers demonstrated that the resolution of the SLF method can be improved substantially by first encoding the homonuclear dipolar decoupling information in the magnetization of the abundant spin (proton) and then transferring it to the magnetization of the rare spin (carbon) through cross polarization (*22–25*). They call the method proton-detected local field spectroscopy (PDLF) because in the earliest version the NMR signal was detected by observing the proton magnetization (*22*). In later versions, including extensions to 3D methods (*24, 35*), the rare spin (^{13}C) magnetization is detected. In order to avoid misunderstanding, we prefer to call the method proton-encoded local field (PELF) spectroscopy. The original PELF method uses MREV-8 for proton dipolar decoupling during the evolution period (*22–25*). Because of the outstanding performance of the BLEW-48 sequence, we proceeded to incorporate it to the PELF method. The modification needed for the successful implementation of the pulse sequence is presented here, and the results of using MREV-8 and BLEW-48 are compared.

For MREV-8, Eq. [1] shows that the effective field direction is in the *xz* plane and forms a 45° angle with the two axes. In order to rotate the proton magnetization to a plane perpendicular to this direction, two 45° *y* pulses are inserted before and after the MREV-8 pulses in the 2D PELF sequence (*22–25*).

For BLEW-48, the Zeeman part of the average Hamiltonian is (*7*)

$$\bar{H}_z^{(0)} = -\frac{4}{3\pi}\sum_i I_{yi}\cdot(\omega_0 - \omega_i). \qquad [3]$$

Since the effective field direction is along the *y* axis, the 45° pulses are not needed. However, because the BLEW-48 sequence is applied in the evolution period after a 90° excitation pulse, its first element (a 90° *x* pulse) must be moved to the end. For phase cycling, the excitation pulse as well as the whole BLEW-48 sequence are phased-shifted by 180° in alternate scans. The complete PELF pulse sequence using BLEW-48 is shown in Fig. 2, and the phase cycles are listed in Table 2. For efficient broadband decoupling, a new sequence called SPARC-16 (*36*) was used in the acquisition period.

The ^{13}C spectra of 5CB using BLEW-48 for proton dipolar decoupling in SLF and PELF are displayed in Fig. 3, which clearly shows that the spectral resolution of the PELF method is much better than that of the traditional SLF method (it should be noted that the spectral width for the PELF spectra is only half of the SLF spectra in Fig. 3). The main reason for the difference in the linewidths is the following.

In the SLF method, the C–H splittings appear as multiplets

TABLE 2
Phase Cycles[a] Used in the PELF Sequence Shown in Fig. 2

	$\pi/2$	BLEW-48[b]	π	BLEW-48[b]	CP	$\pi/2$	$\pi/2$	Acquisition
I-spin	A	A	1	A	1	—	—	I–S decoupling[c]
S-spin	—	—	B	—	C	0	D	Receiver: D

[a] A = 02020202; B = 00220022; C = 00002222; D = 02022020; with 0 = 0°; 1 = 90°, 2 = 180°.
[b] The first normal BLEW-48 element (ref. *7*) is shifted to the end.
[c] Ref. *36*.

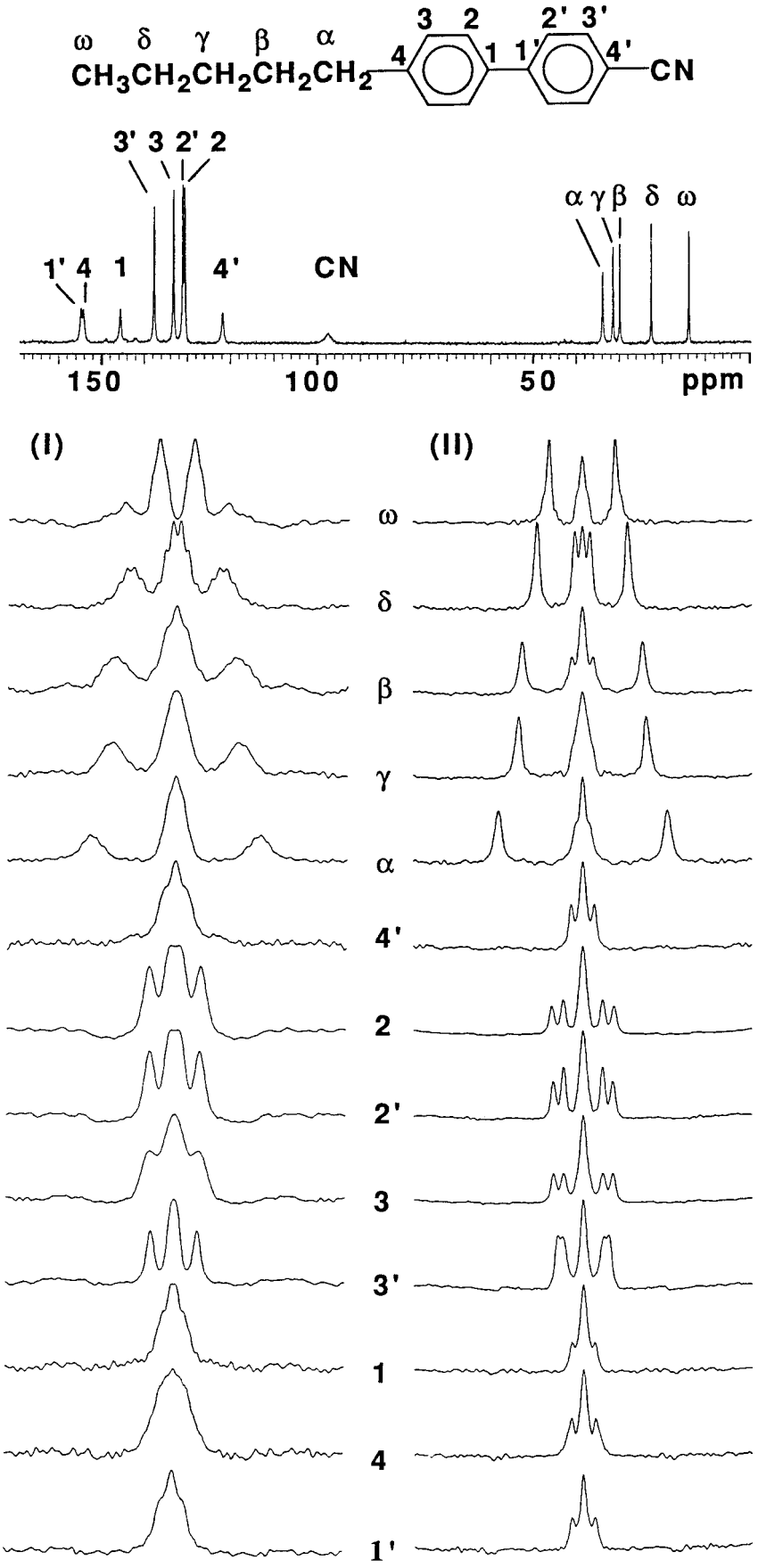
ω δ γ β α
CH3CH2CH2CH2CH2
3 2 2' 3'
4 1 1' 4'
CN
3' 3 2' 2
1' 4 1 4' CN
α γ β δ ω
150 100 50 ppm
(I)
(II)
ω
δ
β
γ
α
4'
2
2'
3
3'
1
4
1'

TABLE 3
C–H Dipolar Coupling Constants[a] (in Hertz) of 5CB at 21°C Obtained from Three Different Methods

Carbon number	SLF with BLEW-48		PELF with BLEW-48		PELF with MREV-8	
1		923 ± 61		862 ± 13		929 ± 18
2	1788 ± 15	−1505 ± 13	1789 ± 17	−1445 ± 16	2042 ± 28	−1559 ± 27
3	1688 ± 17	−1500 ± 19	1712 ± 47	−1383 ± 73	1916 ± 29	−1570 ± 38
4		[b]		919 ± 20		924 ± 40
1′		842 ± 50		873 ± 24		952 ± 33
2′	1634 ± 14	−1439 ± 13	1667 ± 24	−1415 ± 31	1936 ± 40	−1601 ± 32
3′	1375 ± 11	−1469 ± 12	1382 ± 40	−1447 ± 60	1629 ± 16	−1650 ± 29
4′		904 ± 100		862 ± 10		942 ± 35
α	5654 ± 55	[b]	5731 ± 48	319 ± 31	6197 ± 54	542 ± 40
β	3908 ± 40	[b]	3968 ± 33	791 ± 23	4386 ± 51	860 ± 42
γ	4171 ± 50	[b]	4255 ± 38	678 ± 61	4648 ± 39	773 ± 13[c]
						339 ± 17[c]
δ	2942 ± 35	559 ± 6	2917 ± 25	541 ± 26	3229 ± 30	642 ± 114
ω	2041 ± 28	[b]	2048 ± 20	399 ± 60	2325 ± 22	[b]

[a] For each method, values in the first column are for directly bonded C–H pairs; values in the second column are for indirectly bonded C–H pairs. The signs of the indirect C–H dipolar coupling constants for the aliphatic carbons are uncertain.
[b] Unresolved.
[c] There are two sets of long-range couplings (see Fig. 4, IIa).

of multiplets. For example, the ^{13}C peak of the δ-carbon is split by the two directly attached protons into a triplet, each component of which is in turn split by the indirectly bonded protons in the methyl group into a quartet. However, for other aliphatic carbons, the long-range C–H couplings are unresolved and only contribute to line broadening. For all the protonated aromatic carbons, each ^{13}C signal appears as an overlapping doublet of doublets due to splittings caused by the directly bonded and *ortho* protons, respectively. For the quaternary carbons, the C–H splittings caused by the *ortho* protons are smaller, and result in overlapping triplets. Thus, the spectra in Fig. 3, column I, show that the splittings caused by directly and indirectly bonded protons lead to overlapping peaks. On the other hand, each set of C–H splitting in the PELF method appears as a discrete doublet, regardless of the number of equivalent protons attached to the carbon (*22–25*). Thus, long-range couplings yield pairs of peaks with smaller splittings rather than causing line broadening. Very small splittings that cannot be resolved contribute to the central peak. Because of the smaller linewidths of the PELF spectra, C–H splittings can be measured more accurately, and values of some of the long-range couplings can be extracted from the central part of each spectrum by least-squares curve fitting. Once the values of the splittings $\Delta\nu_{ij}$ are determined, the C–H dipolar coupling constants D_{ij} can be calculated by using the equation (*18, 19*)

$$\Delta\nu_{ij} = f \cdot [(3\cos^2\beta - 1) \cdot D_{ij} + J_{ij}], \qquad [4]$$

where f is the scaling factor of the dipolar decoupling sequence, β is the angle between the spinning axis and B_0, and J_{ij} is the C–H scalar coupling constant. The anisotropy in $J_{\text{C–H}}$ is considered to be negligible, and the isotropic $J_{\text{C–H}}$ values for 5CB were determined previously (*37*). The signs of $\Delta\nu_{ij}$ cannot be determined from the spectra; they are assigned based on geometric considerations of the 5CB molecule. The results of the calculated $D_{\text{C–H}}$ values are listed in Table 3, which also includes data obtained from using the MREV-8 sequence in PELF. For comparison, several slices of the 5CB spectra obtained by using the BLEW-48 and MREV-8 sequences are shown in Fig. 4. The results show that, even though MREV-8 does not give as good a resolution as BLEW-48 for the case of benzene dissolved in liquid crystalline solvents (Fig. 1), the application of the two sequences in PELF give comparable spectra for 5CB. The most likely reason is that bulk liquid crystals have considerably broader ^{13}C peaks than small solute molecules. Actually, because the MREV-8 sequence has a larger scaling factor than BLEW-48, some of the smaller splittings are better resolved (Figs. 4a and 4d).

The data in Table 3 show that the dipolar coupling constants obtained from SLF and PELF using BLEW-48 agree with each

FIG. 3. ^{13}C NMR of 5CB at 9.4 T and 21°C, spinning at 1.1 kHz at an angle of 48.5°. *Top:* 1D spectrum; *column I:* 2D SLF slices in the ω1 dimension, spectral width = 3200 Hz; *column II:* 2D PELF slices in the ω1 dimension; spectral width = 1600 Hz. Both methods used BLEW-48 dipolar decoupling in the evolution period. The decoupler power $\gamma B_2/2\pi$ (in kilohertz) was set to 67 for the preparation and refocusing pulses, 38 for BLEW-48, and 20 for cross-polarization and broadband decoupling. A line broadening factor of 10 Hz was used for data processing in both dimensions. Number of scans = 32; Number of increments in the t1 dimension = 64; acquisition time = 0.057 s; relaxation delay time = 3.5 s; each set of 2D spectra was obtained in 2 h.

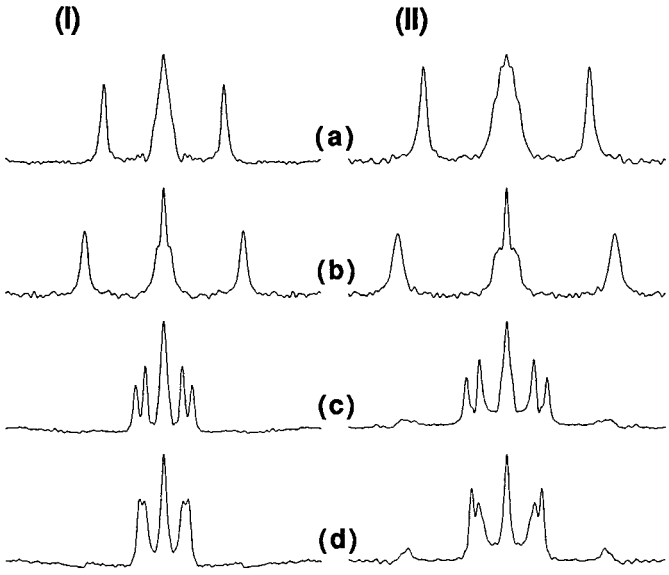

FIG. 4. ^{13}C NMR of 5CB at 9.4 T and 21°C, spinning at 1.1 kHz at an angle of 48.5°, showing several 2D PELF slices in the $\omega 1$ dimension; spectral width = 1600 Hz. (a) γ-carbon; (b) α-carbon; (c) 2′-carbon; (d) 3′-carbon. *Column I:* with BLEW-48 dipolar decoupling in the evolution period; *column II:* with MREV-8 dipolar decoupling in the evolution period. The experimental conditions were the same as those described in the legend of Fig. 3.

other within experimental error, which is expected. However, because the SLF spectra are much broader, the D_{ij} values for the quaternary carbons have larger errors. In fact, the peak for the 4-carbon (Fig. 3, column I) is so broad that the splitting could not be obtained from fitting the spectrum. For PELF using MREV-8 decoupling, the D_{ij} values are all higher than those obtained using BLEW-48 by about 10%, which is larger than the experimental errors for most of the data. In our experiment, the MREV-8 cycle time was set to be 14.9 times the pulse width, yielding a scaling factor of 0.523 (Eq. [2]). If the scaling factor is arbitrarily adjusted to 0.575, the calculated values of D_{ij} become consistent with those obtained using BLEW-48. In view of the better performance of the BLEW-48 sequence for homonuclear dipolar decoupling (*7, 18, 19*; Fig. 1), we consider that its application to PELF would also give more reliable data than MREV-8. Furthermore, the peaks obtained from the use of BLEW-48 show less lineshape distortion and spurious signals (Figs. 4c and 4d); their linewidths are also smaller, so that they have better signal-to-noise ratios. The imperfections in using MREV-8 can be minimized by meticulous adjustment of the pulse spacing, but it is less convenient for routine experimental studies. On the other hand, because BLEW-48 is a windowless sequence and can be readily incorporated into the evolution period with a waveform generator rather than actually turning the decoupler on and off between pulses, it is affected less by pulse imperfection.

The cycle time of BLEW-48 is $48 \cdot \tau_\omega$, which is quite long. However, we found that it is not necessary to set the increments in the evolution period in multiples of a whole BLEW-48 cycle; increments in steps of $\frac{1}{4}$ or $\frac{1}{2}$ of a full cycle give the same result. Therefore, the spectral width in the $\omega 1$ dimension of the PELF method is not limited by the length of the BLEW-48 cycle.

In conclusion, we have shown that the windowless BLEW-48 homonuclear dipolar decoupling sequence gives the best resolution for the ^{13}C spectra of benzene dissolved in liquid crystal solvents. It is also applicable to the powerful 2D PELF method for the study of bulk liquid crystals, and it may be preferable to the standard MREV-8 sequence.

ACKNOWLEDGMENTS

This work was supported by the National Science Foundation under Grant nos. DMR-9700680 and OST-9550478. The authors are grateful to Dr. Lyndon Emsley for providing the PELF/MREV-8 pulse program listing for the Varian spectrometer system.

REFERENCES

1. M. Lee and W. I. Goldburg, *Phys. Rev. A* **140,** 1261 (1965).
2. J. S. Waugh, L. Huber, and U. Haeberlen, *Phys. Rev. Lett.* **20,** 180 (1968).
3. U. Haeberlen, and J. S. Waugh, *Phys. Rev. A* **175,** 453 (1968).
4. P. Mansfield, *J. Phys. C* **4,** 1444 (1971).
5. W.-K. Rhim, D. D. Elleman, and R. W. Vaughn, *J. Chem. Phys.* **59,** 3740 (1972).
6. D. P. Burum and W.-K. Rhim, W.-K. *J. Chem. Phys.* **71,** 944 (1979).
7. D. P. Burum, N. Linder, and R. R. Ernst, *J. Magn. Reson.* **44,** 173 (1981).
8. K. Takegoshi and C. A. McDowell, *Chem. Phys. Lett.* **116,** 100 (1985).
9. H. Liu, S. J. Glaser, and G. P. Drobny, *J. Chem. Phys.* **93,** 7543 (1990).
10. J. H. Iwamiya, S. W. Sinton, H. Liu, S. J. Glaser, and G. P. Drobny, *J. Magn. Reson.* **100,** 367 (1992).
11. A. Bielecki, A. C. Kolbert, and M. H. Levitt, *Chem. Phys. Lett.* **155,** 341 (1989).
12. A. Bielecki, A. C. Kolbert, H. J. M. de Groot, R. G. Griffin, and M. H. Levitt, *Adv. Magn. Reson.* **14,** 111 (1990).
13. M. Hohwy, and N. C. Nielsen, *J. Chem. Phys.* **106,** 7571 (1997).
14. M. Hohwy, P. V. Bower, H. J. Jakobsen, and N. C. Nielsen, *Chem. Phys. Lett.* **273,** 297 (1997).
15. R. G. Pembleton, L. M. Ryan, and B. D. Gerstein, *Rev. Sci. Instrum.* **48,** 1286 (1977).
16. L. M. Ryan, R. E. Taylor, A. J. Paff, and B. D. Gerstein, *J. Chem. Phys.* **72,** 508 (1980).
17. G. E. Maciel, C. E. Bronmimann, and B. L. Hawkins, *Adv. Magn. Reson.* **14,** 125 (1990).
18. B. M. Fung, *J. Magn. Reson.* **66,** 525 (1986).
19. B. M. Fung, *J. Magn. Reson.* **72,** 353 (1987).
20. J. Courtieu, J.-P. Bayle, and B. M. Fung, *Progr. NMR Spectroscopy* **26,** 141 (1994).
21. B. M. Fung, "Liquid Crystalline Samples: Carbon-13 NMR," in Encyclopedia of Nuclear Magnetic Resonance (D. M. Grant and R. K. Harris, Eds.), pp. 2744–2751, Wiley, Chichester, U.K. (1996).

22. K. Schmidt-Rohr, D. Nanz, L. Emsley, and A. Pines, *J. Phys. Chem.* **98,** 6668 (1994).

23. M. Hong, K. Schmidt-Rohr, and A. Pines, *J. Am. Chem. Soc.* **117,** 3310 (1995).

24. M. Hong, A. Pines, and S. Caldarelli, *J. Phys. Chem.* **100,** 14815 (1996).

25. S. Caldarelli, M. Hong, M., L. Emsley, and A. Pines, *J. Phys. Chem.* **100,** 18696 (1996).

26. C. H. Wu, A. Ramamoorthy, and S. J. Opella, *J. Magn. Reson. A* **109,** 270 (1994).

27. A. Ramamoorthy and S. J. Opella, *Solid State NMR* **4,** 387 (1995).

28. J. S. Waugh, *Proc. Natl. Acad. Sci. USA* **73,** 1394 (1976).

29. R. K. Hester, J. L. Ackerman, B. L. Neff, and J. S. Waugh, *Phys. Rev. Lett.* **36,** 1081 (1976).

30. J. S. Waugh and S. J. Opella, *J. Chem. Phys.* **66,** 4919 (1977).

31. E. R. Rybaczewski, B. L. Neff, J. S. Waugh, and J. S. Sherfinsky, *J. Chem. Phys.* **67,** 1231 (1977).

32. E. Guittet, D. Piveteau, M.-A. Delsuc, and J.-Y. Lallemand, *J. Magn. Reson.* **62,** 336 (1985).

33. J. Ashida and D. Rice, *Magnetic Moments* (a Varian publication) **8**(1), 19 (1996).

34. B. M. Fung, *J. Magn. Reson.* **86,** 160 (1990).

35. S. A. Caldarelli, A. Lesage, and L. Emsley, *J. Am. Chem. Soc.* **118,** 12224 (1996).

36. Y. Yu and B. M. Fung, *J. Magn. Reson.* **130,** 317 (1998).

37. C.-D. Poon, J. Afzal, and B. M. Fung, *Magn. Reson. Chem.* **24,** 1014 (1986).